Tree Physiology 31, 637–648
doi:10.1093/treephys/tpr047

Research paper

Hydraulic adjustments underlying drought resistance of *Pinus halepensis*

Tamir Klein[1,3], Shabtai Cohen[2] and Dan Yakir[1]

[1]Department of Environmental Sciences and Energy Research, Weizmann Institute of Science, Rehovot 76100, Israel; [2]Institute of Soil, Water and Environmental Sciences, Volcani Center ARO, Beit Dagan 50250, Israel; [3]Corresponding author (tamir.klein@weizmann.ac.il)

Received January 5, 2011; accepted April 26, 2011; published online June 27, 2011; handling Editor Roberto Tognetti

Drought-induced tree mortality has increased over the last decades in forests around the globe. Our objective was to investigate under controlled conditions the hydraulic adjustments underlying the observed ability of *Pinus halepensis* to survive seasonal drought under semi-arid conditions. One hundred 18-month saplings were exposed in the greenhouse to 10 different drought treatments, simulating combinations of intensities (fraction of water supply relative to control) and durations (period with no water supply) for 30 weeks. Stomata closed at a leaf water potential (Ψ_l) of −2.8 MPa, suggesting isohydric stomatal regulation. In trees under extreme drought treatments, stomatal closure reduced CO_2 uptake to −1 µmol m^{-2} s^{-1}, indicating the development of carbon starvation. A narrow hydraulic safety margin of 0.3 MPa (from stomatal closure to 50% loss of hydraulic conductivity) was observed, indicating a strategy of maximization of CO_2 uptake in trees otherwise adapted to water stress. A differential effect of drought intensity and duration was observed, and was explained by a strong dependence of the water stress effect on the ratio of transpiration to evapotranspiration T/ET and the larger partitioning to transpiration associated with larger irrigation doses. Under intense or prolonged drought, the root system became the main target for biomass accumulation, taking up to 100% of the added biomass, while the stem tissue biomass decreased, associated with up to 60% reduction in xylem volume.

Keywords: carbon reallocation, drought tolerance, embolism, transpiration ratio, tree mortality.

Introduction

Water deficiency is the main factor limiting plant production worldwide (Boyer 1982, Flexas et al. 2004) and drought is an important driver of eco-physiological adaptations in plants. Future climate warming is expected to elevate atmospheric water demand; however, changes will not be restricted to increases in mean temperature, but will also include increases in the frequency and intensity of droughts (Christensen et al. 2007, Seager et al. 2007, Sterl et al. 2008). The fate of many forest ecosystems will depend on the ratio of the rate of the climate changes to the rate of adaptation to such changes. A ratio larger than one means that the rate of climate change exceeds the rate of plant adaptation. Accumulating evidence of drought-induced tree mortality in recent years (Allen et al. 2009 and references therein) might be the result of this scenario.

Forest function under drought has been studied intensively in semi-arid pine afforestation in Southern Israel for the past decade, indicating relatively high forest productivity (Grunzweig et al. 2007). This was associated with adjustments to the dry conditions, such as a shift in maximum assimilation rates to early spring (Maseyk et al. 2008, Rotenberg and Yakir 2010). It was also shown that low rates of water loss were associated with increasing sensitivity of stomatal conductance (g_s) to soil moisture below a relative extractable water (REW) value of 0.4, and decreased g_s sensitivity to vapor pressure deficit (VPD) below a REW of 0.2. These eco-physiological responses raise questions concerning the underlying hydraulic mechanisms allowing the trees to withstand regular long and intense drought periods.

In natural ecosystems, drought is typically driven by restriction in either the amount or the frequency of precipitation. This entails a dual parameterization of drought. While the reduction in precipitation amount below a certain threshold (e.g., the negative deviation from a multi-annual average) defines drought intensity, the reduction in precipitation frequency defines drought interval (IPCC 2001). Together, these two parameters determine the drought impact on the ecosystem and agricultural productivity of the affected region. High-intensity drought episodes, consequently bearing a profound impact on forest and plant function, have been studied extensively (Breshears et al. 2005, Ciais et al. 2005). Yet the distinction of drought interval as an equally important drought parameter has been described only in a few studies (e.g., Mueller et al. 2005), in spite of the fact that it plays a major role in determining responses in semi-arid ecosystems, where precipitation often arrives in sporadic events, which can be described as pulses.

Plant resistance to drought relies on two hypothetical contrasting physiological approaches: drought avoidance and drought tolerance. The underlying mechanism of either approach involves stomatal response and regulation of water status, named isohydric or anisohydric, respectively (Tardieu and Simonneau 1998, McDowell et al. 2008). Isohydric plants reduce g_s as soil and atmospheric conditions dry, maintaining relatively constant leaf water potential regardless of drought intensity. Anisohydric species, in contrast, allow leaf water potential to decline as soil water potential declines with drought (West et al. 2008). The soil–tree–atmosphere continuum also includes the tree hydraulic system, from the water uptake sites at the root hairs, up the xylem conduits in the stem and on to the transpiration sites in the leaf stomata. Water is transported through this system following a water potential (Ψ) gradient which considerably increases with drought. Both approaches enable plant survival under harsh drought conditions; however, each has an inherent pitfall that can lead to failure in certain conditions. Prolonged reductions of g_s expose isohydric species to carbon starvation, while very negative leaf water potentials in anisohydric species result in xylem cavitation and embolism and subsequent hydraulic failure (McDowell et al. 2008). A basic risk assessment of these mechanisms reveals that not only drought intensity but also the duration of drought plays a key role in determining the fate of the plant.

Aleppo pine (*Pinus halepensis* Miller) is an important forest tree in the Mediterranean region, and the only pine species native to Israel (Quezel 2000). Temperature and precipitation requirements generally confine its distribution to sub-humid areas of the Mediterranean. In light of predictions of global drying and warming for this region, there is some concern about the physiological ability of *P. halepensis* to persevere in large afforestations in the future (Oliveras et al. 2003, Maestre and Cortina 2004). This ability mainly depends on the hydraulic properties of *P. halepensis*, which have already attracted the attention of several research programs in Mediterranean countries. Under induced drought, seedlings of Italian *P. halepensis* ecotypes from more xeric habitats had greater g_s and transpiration (T) rates than ecotypes from more mesic habitats (Tognetti et al. 1997). A subsequent trial (Calamassi et al. 2001) on younger seedlings of European ecotypes confirmed this observation, and added that the 'xeric' ecotypes displayed strategies typical of drought-tolerant species. Associations between the hydraulic characteristics and tree function were the focus of another study (Royo et al. 2001), which showed that growth parameters (e.g., height, diameter) of young seedlings in the greenhouse were very sensitive to the irrigation regime. Yet after planting in the field under natural conditions, differences diminished and became insignificant, suggesting that the hydraulic systems of *P. halepensis* are highly plastic. Assessments of vulnerability to xylem embolism, together with field measurements of leaf water potential, led to predictions of high values (>75%) of xylem embolism under drought (Oliveras et al. 2003). However, the authors concluded, also in contrast to earlier studies (Calamassi et al. 2001, Atzmon et al. 2004), that *P. halepensis* is a drought-avoiding species. A parallel comparative study confirmed this conclusion by analysis of carbon isotope discrimination in tree rings (Ferrio et al. 2003). While these works provided ample information, results and interpretations regarding the hydraulic regulation in *P. halepensis* varied. Perhaps one of the reasons for this is the lack of a mechanistic description of hydraulic regulation in *P. halepensis*. Such a description will have to include the underlying mechanism, i.e., the type of stomatal regulation of water status, and tie it to the relevant physiological processes. To accomplish this goal, more complex drought scenarios must be tested, robust techniques must be used, and the use of very young seedlings should be limited.

Based on field observations, we hypothesize that the mode of stomatal regulation in *P. halepensis* is isohydric. Yet this gives rise to additional questions, e.g., how is carbon uptake sustained under long drought, and how is the tree water supply ensured so as to postpone stomatal closure. By integrating a mechanistic approach, combining high-resolution measurements and using state-of-the-art methodology, we wish to deepen our understanding of water use by forest trees under drought. Ultimately this should facilitate forestry planning in the face of contemporary challenges, i.e., global warming and drying in many regions.

Materials and methods

Plant material

Pinus halepensis trees were grown from seed (source: Mount Carmel, Israel) in 4 cm diameter cylinders in Styrofoam blocks at KKL-JNF Eshtaol nursery. In February 2009 one hundred 16-month saplings with a height to meristem of 44.6 ± 4.2 cm and a root collar diameter of 3 ± 0.4 mm were taken from one block. In April 2009 trees were transplanted into 5 l pots at the Weizmann Institute of Science greenhouse facility in Rehovot. Young trees were kept under optimal growth conditions (ambient light, 24 °C, RH = 70%, ultra-optimal irrigation) for a 3-week acclimation period.

Experimental set-up and design

The experiment was on 100 actively growing 18-month trees in 5 l pots. Trees were divided into 10 irrigation treatments as shown in Table 1, 10 trees per treatment. A 3-week pilot trial characterized the tree water requirement under greenhouse conditions to be 350 ml week^{-1} per pot. This was used as the standard 100% irrigation amount (A_0) given once a week to trees in the control group. The water portion given in a treatment (A_i) was 75, 50 or 25% of that, creating four discrete levels of drought intensity. Treatments differed also in the duration of their drought cycle, which was 7, 14 or 21 days. This means that while control trees had three irrigation events in 21 days (D_0), the number of irrigation events given in a treatment (D_i) was 3, 1.5 or 1 in 21 days (Table 1). Treatments are indicated by their index number (T1–T9) and their respective irrigation regime (*x*:*y*, where *x* is amount, in % of control, and *y* is time between irrigations, in weeks). Trees were grown together in one greenhouse over a 30-week period. Other environmental factors (air temperature (T), relative humidity (RH), photosynthetically active radiation (PAR)) were maintained at reasonable conditions for young tree growth. Average T was 22 ± 6.5 °C and average RH was 71 ± 15%.

Soil and water parameters, including soil salinity

Pots contained 20 cm deep enriched sandy loam on top of a 2 cm gravel infiltration layer. Soil water content (SWC) was determined by the oven-drying method on samples taken three times in the course of the experiment. Every pot was weighed twice a week (morning and evening of the same day) using a Sartorius 3808 MP8 wide-range balance (up to 30 kg with 0.1 g precision; Gottingen, Germany). Calibration of pot mass values with periodic measurements of SWC allowed its determination for every week along the experiment. The long-term hydrological balance of a system can be represented by

$$S = D + R + \mathrm{ET} \qquad (1)$$

where S is supply inputs (precipitation and irrigation), D is drainage, R is runoff and ET is evapotranspiration. While Eq. (1) provides the overall hydraulic perspective, in our experiment the relatively small irrigation amounts were found to result in D and R being below detection limits, and at the experimental time-scale measurements of SWC indicated that SWC declined continuously (Figure 1a). Over this time-scale $\mathrm{ET} > S$ and ET was therefore quantified from

$$\mathrm{ET}_j = W_{j-1} - W_j + S_j \qquad (2)$$

where ET in week *j* was calculated from the difference in pot weight (*W*, measured each Thursday at 18:30, prior to irrigation) between week *j* and the previous week (*j* – 1) plus the irrigation supplied during the past week (*S*j). Mean weekly ET, which was calculated for each treatment, was further used in the analysis (Table 1). In order to check whether the drought

Table 1. Summary of treatments and hydrological components of the 30-week experiment. Treatments are indicated by their index number (T1–T9) and their respective irrigation regime (*x*:*y*, where *x* is amount, in % of control, and *y* is time between irrigations, in weeks). *A* indicates amount of irrigation water; *D* indicates number of irrigation events in 3 weeks (control, Ctrl, treatment was irrigated weekly); D_i/D_0 indicates the irrigation frequency of treatment *i* relative to control ($D_0 = 3$); *S* indicates total water supply; T and ET indicate transpiration and evapotranspiration, respectively; PDI indicates plant drought index, as defined in Eq. (4). Note that ETj > *S*j because the initial, standard, pot water content was not included in *S*.

	Ctrl	T1	T2	T3	T4	T5	T6	T7	T8	T9
	1:1	0.75:1	0.75:2	0.75:3	0.5:1	0.5:2	0.5:3	0.25:1	0.25:2	0.25:3
A (g)	350	262.5	262.5	262.5	175	175	175	87.5	87.5	87.5
A_i/A_0	1.00	0.75	0.75	0.75	0.50	0.50	0.50	0.25	0.25	0.25
D	3	3	1.5	1	3	1.5	1	3	1.5	1
D_i/D_0	1.00	1.00	0.50	0.33	1.00	0.50	0.33	1.00	0.50	0.33
*S*i	1.00	0.75	0.38	0.25	0.50	0.25	0.17	0.25	0.13	0.08
$\mathrm{T}_i/\mathrm{ET}_i$	0.18	0.21	0.22	0.24	0.16	0.19	0.22	0.09	0.13	0.15
PDI	0.00	0.14	0.55	0.67	0.54	0.74	0.79	0.88	0.92	0.91
*S*j (g week^{-1})	350	263	131	88	175	88	58	88	44	29
ETj (g week^{-1})	366	291	157	93	197	113	72	116	71	56
*T*j (g week^{-1})	67	60	34	22	32	21	16	10	9	10

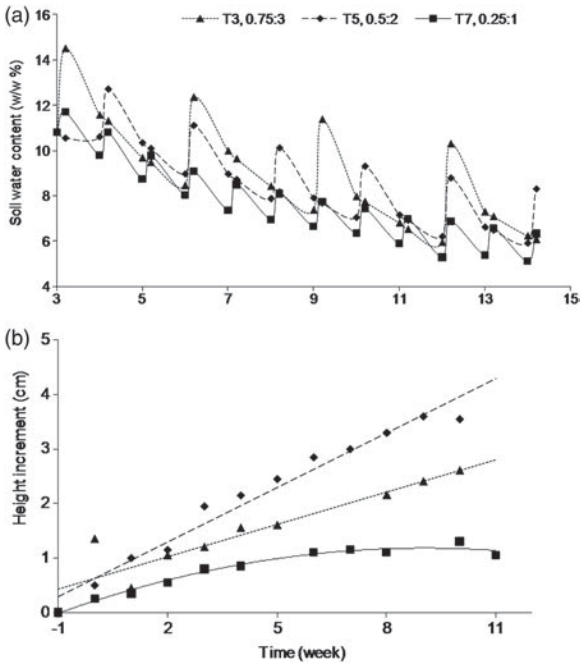

Figure 1. Changes in SWC (a) and tree height (b) with time during the drought experiment, for treatments with identical total irrigation amounts: T3, T5 and T7 ($n = 10$). Height measurements started before the onset of the experiment (last simultaneous irrigation to all treatments). Equations of the regression lines were $y = 0.33x + 0.63$, $R^2 = 0.97$ for T3; $y = 0.20x + 0.62$, $R^2 = 0.86$ for T5; and $y = 0.01x^2 + 0.21x + 0.21$, $R^2 = 0.98$ for T7. Saplings were 1.5 years old.

effect was confounded by a salinity effect, electrical conductivity (EC) of the soil and irrigation water was determined with a YSI 3200 EC meter (Yellow Springs, OH, USA). Average EC of irrigation water (tap water at the Weizmann Institute) was 0.8 dS m^{-1}, indicating a very 'slight salinity problem' according to the Food and Agriculture Organization of the United Nations irrigation guidelines (Ayers and Westcot 1985). At the end of the experiment, 5 g soil samples were taken from pots of control or T9 (0.25:3) trees and thoroughly mixed with 5 g of double-distilled water. Slurries were shaken at 200 rpm for 2 h followed by centrifugation and EC was determined as described above. Average EC values of the slurries ranged from 0.35 dS m^{-1} for soil from control pots to 1.4 dS m^{-1} for soil taken from pots from the lowest irrigation (T9). Since *P. halepensis* is salt tolerant at levels of 6–8 dS m^{-1} (Miyamoto et al. 2004), this indicates that soil salinity was not a major factor affecting plant physiology in this experiment.

Morphological measurements and biomass accumulation

During the course of the experiment, height to meristem and root collar diameter were measured for all trees once a week. At the end of the experiment, trees were dissected; root system and leaves were carefully collected and laid out inside transparent plastic bags and scanned using a Toshiba e-studio 282 scanner (Toshiba Corp., Tokyo, Japan). Scanned images were analyzed using GNU image manipulation program 2.6 (www.gimp.org) to give total projected root and leaf area estimates. Detached root systems were also used for measurement of root volume by the water displacement method using a collection tube attached to a nozzle-fitted Erlenmeyer flask. Upon initiation of the experiment, five additional trees were sacrificed; root systems were cleaned from soil particles and cut from the stem, and needles were collected. The three fractions (leaves, stem and roots) were dried at 60 °C for 48 h and later weighed on a Precisa 62A balance (Precisa Gravimetrics, Dietikon, Switzerland) to give the dry mass of each fraction. By the end of the experiment the dry mass of each fraction was determined for each tree. The increase in biomass over time was calculated by subtracting mean initial dry mass from final dry mass.

Leaf gas exchange and water potential

During the course of the experiment, leaf gas exchange, i.e., stomatal conductance (g_s), transpiration (T) and net assimilation (A_n), were measured once a week on three trees per treatment. Measurements were made on a pre-marked twig terminus carrying juvenile needles with a total projected area of 2 cm^2, using a LI-6400 Photosynthesis System (Licor Inc., Lincoln, NE, USA) equipped with an LED lamp set to 1000 μmol m^{-2} s^{-1} PAR. This PAR value was shown as saturating by light response curves of seedlings of three Mediterranean pine species (Awada et al. 2003). Mean weekly amounts of transpiration (T_j, g week^{-1}) were estimated from leaf-level measurements according to

$$T_j = T_{\mathrm{mean}} \times t_{\mathrm{T}} \times k \times \mathrm{MW_w} \times \{L_{\mathrm{a}\,j-1} + [(L_{\mathrm{a\,week30}} - L_{\mathrm{a\,week0}})/40]\} \qquad (3)$$

where T_{mean} is an average of three transpiration measurements (in mmol m^{-2} s^{-1}) between 8:00 and 12:00, t_{T} is the cumulative time (in s) of transpiration during the week (assuming 12 h/day), k is a correction factor that was used to account for the fact that T was measured at least 1 week after each irrigation event (thereby underestimating T by a factor of 2), $\mathrm{MW_w}$ is the molar mass of water (18 g mol^{-1}), and L_{a} is the calculated leaf area based on measurements at the beginning ($L_{\mathrm{a\,week0}}$) and end ($L_{\mathrm{a\,week30}}$) of the experiment and assuming a linear increase in between. Once in 1 or 2 weeks gas exchange measurements were accompanied by measurements of leaf water potential (Ψ_l) using the pressure chamber technique (Scholander et al. 1965; Holbrook et al. 1995). Small (5–7 cm long) twigs were cut from the same trees used for the gas exchange measurements (three per treatment) and put in a pressure chamber (Arimad 2; A.R.I., Kfar Charuv, Israel) fed by a nitrogen gas cylinder and equipped with a lamp-carrying magnifying glass. Gas pressure within the chamber was gradually increased (~1 MPa min^{-1}) until water emerged from the protruding cut branch surface, and the pressure value was recorded as leaf water potential (Ψ_l).

Xylem hydraulic conductivity

Hydraulic conductivity was measured in five to nine trees per treatment, under low pressure (0.02 MPa) before and after perfusing the xylem tissue at a high pressure of 0.5 MPa. In order to eliminate variations at the time of sampling due to the treatment-specific irrigation program, trees were watered 24 h prior to measurement. We can assume that any reversible reductions in conductance were not measured and the measurement captured the mid-term steady-state developmental responses (and not short-term embolism). A 30 cm stem section was cut from the base of the stem and resin secretion from the cuts was eliminated by placing both ends (5 cm from cut tips) in a water bath at 95 °C for 10 min (adapted from Waring and Silvester 1994). Next, stem sections were submerged in distilled water for 10 min. The root collar end of each stem was then fitted with a rubber gasket, while still submerged, to a latex pipe fed by 10 mM KCl solution in a double-distilled water reservoir. A hydrostatic pressure of 0.02 MPa was applied by placing the reservoir exactly 2 m above the stem section. For 2 h, water dripping from the distal end of the stem section was collected and weighed every 20 min. The water flow rate (kg s^{-1}) was divided by the pressure gradient (0.02 MPa) along the 30 cm stem length to provide the hydraulic conductivity K_h (kg m MPa^{-1} s^{-1}), as described by Tyree and Alexander (1993). K_h was further divided by the xylem cross-sectional area to provide the specific hydraulic conductivity K_s (kg m^{-1} MPa^{-1} s^{-1}). Stem sections (1–4 per treatment) were then fitted with a high-pressure valve to a pressure-resistant pipe fed by 10 mM KCl solution reservoir placed inside a Scholander pressure chamber. Pressurizing the solution through the segment at 0.5 MPa for 5 min followed by a second measurement of K_s determined the maximum specific conductivity, $K_{s\ max}$.

Statistical analysis

Data were subjected to analysis of variance (ANOVA) using JMP software (Cary, NC, USA). Measurements of individual trees were used as observations, where drought intensity (water amount) and drought interval (irrigation frequency) were defined as factors. Differences between treatments were considered significant when type 3 sum of squares met the *F*-test criterion at probability <0.05.

Results

Differential effect of drought intensity and duration on tree survival and growth

The differential effect of drought intensity and duration was first assessed by comparing growth rates in T3 (0.75:3), T5 (0.5:2) and T7 (0.25:1) treatments. These treatments had identical total irrigation amounts ($Si = 0.25$), but clearly different growth patterns (Figure 1b). These effects on growth were linked to changes in SWC (Figure 1a): in T7 (0.25:1), the frequent small irrigation doses resulted in increasingly lower SWC values, reflecting the effects of 'drought intensity' (Figure 1b). Comparing T5 and T3 indicated that in this case the higher irrigation dose (T3) was not sufficient to compensate for the 'drought duration' effect (3 weeks vs. 2 weeks), and its mean SWC and growth rates were lower.

We further assessed the observed links between irrigation patterns and SWC by partitioning the ET fluxes. Based on integrated leaf scale gas exchange measurements, mean weekly transpiration (T_j) ranged from 9 to 67 g $week^{-1}$, compared with 56–366 g $week^{-1}$ for ET_j (76–91% of the water demand) depending on the treatment (Table 1). Partitioning between T_i and ET_i was linearly related to the relative water amount at each event (A_i/A_0) for a given drought duration. For example, where drought duration was 1 week, T_i/ET_i of T1 (0.75:1), T4 (0.5:1) and T7 (0.25:1) was 0.21, 0.16 and 0.09, respectively, yielding the regression equation $T_i/ET_i = 0.24 \times A_i/A_0 + 0.03$ ($R^2 = 0.99$). The partitioning ratio increased with A_i/A_0 also under higher drought duration, albeit with lower regression slopes (Figure 2).

To assess the integrated drought intensity/duration effects, a simple empirical plant drought index (PDI) that considers their combined effect was used:

$$\mathrm{PDI} = 1 - S_i \times T_i \,/\, \mathrm{ET}_i \qquad (4)$$

where the relative total water supply in treatment *i*, *Si*, was obtained from $Si = A_i/A_0 \times D_i/D_0$, where A_i is the water amount for the treatment, A_0 is the control amount (which was predetermined as indicated in Materials and methods), and D_i and D_0 are the number of irrigation events in 21 days (maximum drought duration in this study) in a treatment and control,

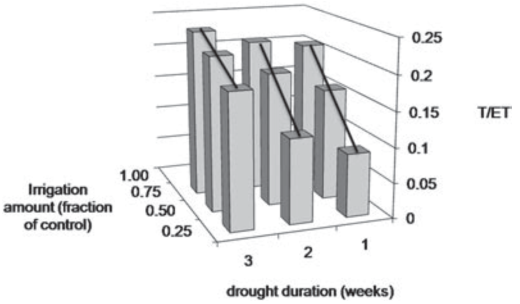

Figure 2. Change in the ratio of transpiration, T, to evapotranspiration, ET (T/ET, transpiration ratio), as a function of irrigation amount (% of control) and drought duration. Equations of the regressions lines were $T/ET = 0.24 \times A_i/A_0 + 0.03$ ($R^2 = 0.99$) for 1 week, $T/ET = 0.20 \times A_i/A_0 + 0.08$ ($R^2 = 0.95$) for 2 weeks and $T/ET = 0.10 \times A_i/A_0 + 0.17$ ($R^2 = 0.99$) for 3 weeks.

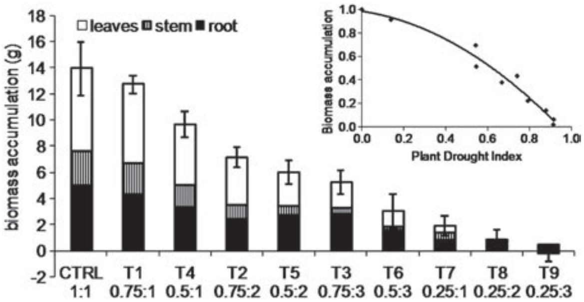

Figure 3. Dry biomass accumulation in leaves, stems and roots, in response to drought treatments (T1–T9; see Table 1). Results were arranged according to the treatment's Plant Drought Index (PDI, Eq. (4)), with total biomass relative to control in response to PDI shown in the inset ($BA = 1 - 0.82 \times PDI^2 - 0.27 \times PDI$). Error bars indicate the standard error of the mean mass in all three organs combined ($n = 6$).

respectively (Table 1; i.e., Si and PDI ranged between zero and 1 with $S = 1$ and $PDI = 0$ for optimal conditions). Weight-based estimates of ET were simplified in our system since runoff, R, and drainage, D, could be ignored (see Eq. (1)) and transpiration (T) rates were calculated based on gas exchange measurements as described above. Within 30 weeks of exposure to drought, all trees receiving 25% of optimal irrigation (T7–T9) died, while if total irrigation input was 50% of optimum, most (60%) trees survived even the lowest irrigation frequency (T6). Accordingly, the threshold PDI value for tree survival was $0.74 < PDI < 0.79$.

Trees started the experiment with ~6 g of biomass, and hence the accumulation of 14 g in control trees means that 230% was the potential growth in the course of the trial (Figure 3). Drought reduced this growth to 50% in T6 (0.5:3) trees, and lower in trees that received only 25% irrigation and died before the end of the trial. The empirical drought index, PDI, predicted well reductions in biomass accumulation (BA, as a fraction of control; Figure 3, $R^2 = 0.97$), yielding the following regression equation:

$$BA = 1 - 0.82 \times PDI^2 - 0.27 \times PDI \qquad (5)$$

The non-linear nature of Eq. (5) suggested that tree growth was less sensitive to drought at low PDI values, but sensitivity increased at high PDI. The differential effects of drought intensity and drought interval were also apparent based on the analysis of variance reported in Table 2.

Response of the tree's hydraulic structure to drought parameters

Root, stem and leaf biomass were measured in order to understand the structural response of each hydraulic component. Figure 3 shows the biomass partitioning for all treatments, ordered according to their PDI value. When water supply was optimal, biomass partitioning to leaves, stem and roots was 50, 20 and 30%, respectively. Biomass distribution was similar for mild drought, in T1 (0.75:1), T2 (0.75:2) and T4 (0.5:1). Under more intense drought, as for T5 (0.5:2), diversion of biomass to roots increased while decreasing to stems, with this trend further increasing in T3 (0.75:3). At the limit of tree survival in

Table 2. Response means for the drought treatments, slopes of linear regression fits and their significance levels, from ANOVA of the parameters indicated, as a function of 'drought duration' (irrigation frequency) and 'drought intensity' (water amount). Responses not connected by the same letter are significantly different. Slopes express a change (percent of control) for each 1-week extension of the drought period or for each 25% reduction in irrigation amount. All measurements were made at the end of the 30-week experiment, except for g_s (Week 8) and height increment (Ht. increm.) and diameter (Week 17).

	Ht. increm. (cm)	Diameter (mm)	Total biomass increm. (g)	Stem biomass increm. (g)	Leaf biomass increm. (g)	Root biomass increm. (g)	K_s (kg m^{-1} MPa^{-1} s^{-1})	g_s (mol m^{-2} s^{-1})	A_r (cm^2)
Means									
Control	5.6^{a}	5.27^{a}	12.20^{a}	2.56^{a}	6.36^{a}	5.01^{a}	0.13^{a}	0.06^{a}	24.6^{ab}
T1	4.7^{ab}	5.20^{ab}	12.20^{a}	2.33^{ab}	6.07^{ab}	4.32^{ab}	0.11^{a}	0.06^{ab}	27.3^{a}
T2	4.4^{abc}	4.55^{cd}	6.49^{bc}	1.08^{cd}	3.61^{cd}	2.45^{cd}	0.05^{a}	0.04^{cd}	19.1^{c}
T3	2.9^{bcde}	4.12^{de}	4.70^{cd}	0.50^{def}	1.96^{ef}	2.79^{cd}	0.04^{a}	0.02^{cde}	25.2^{ab}
T4	4.3^{abc}	4.78^{bc}	9.34^{ab}	1.66^{bc}	4.63^{bc}	3.37^{bc}	0.04^{a}	0.04^{bc}	28.4^{a}
T5	4.0^{abcd}	4.34^{cde}	6.00^{bc}	0.66^{de}	2.60^{de}	2.76^{cd}	0.03^{a}	0.03^{cde}	19.7^{bc}
T6	2.4^{cde}	4.25^{de}	1.92^{de}	0.20^{ef}	1.26^{efg}	1.61^{de}	n.a.	0.01^{de}	18.1^{c}
T7	3.8^{abcd}	4.33^{cde}	1.63^{de}	0.60^{def}	0.50^{fg}	0.80^{e}	n.a.	0.01^{e}	12.8^{d}
T8	2.0^{de}	3.87^{ef}	0.98^{e}	0.01^{ef}	0.10^{g}	0.73^{e}	n.a.	0.01^{e}	11.1^{d}
T9	1.1^{e}	3.65^{f}	0.56^{e}	-0.14^{f}	-0.10^{g}	0.46^{e}	n.a.	0.01^{de}	12.1^{d}
Regression slope									
Duration	–21.9	–8.6	–26.3	–31.9	–26.8	–18.0	–29.1	–22.5	–10.0
Intensity	–17.2	–7.3	–29.4	–27.1	–30.2	–26.4	–35.8	–25.5	–19.9
Significance									
Duration	n.s.	<0.001	<0.001	<0.001	<0.001	<0.005	n.s.	<0.005	<0.05
Intensity	n.s.	<0.01	<0.01	<0.01	<0.05	<0.01	n.s.	<0.05	n.s.

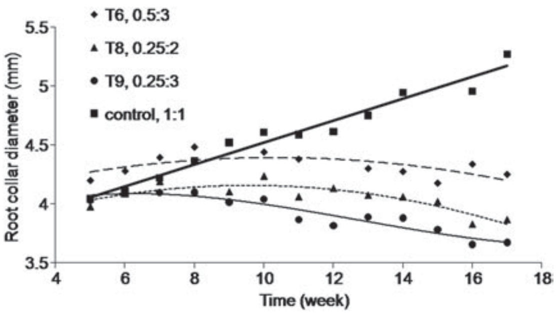

Figure 4. Change with time in mean root collar diameter of trees under drought treatments where biomass allocation to stem was ≤0 and under control treatment ($n = 10$). Equations of regression lines were $y = 0.09x + 3.59$, $R^2 = 0.96$ for control; $y = 0.004x^2 + 0.09x + 3.93$, $R^2 = 0.41$ for T6; $y = 0.006x^2 + 0.11x + 3.61$, $R^2 = 0.77$ for T8; and $y = 0.0004x^3 + 0.016x^2 + 0.15x + 3.66$, $R^2 = 0.89$ for T9.

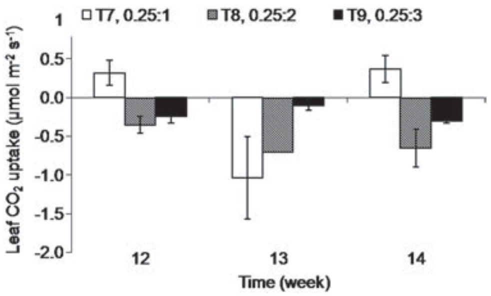

Figure 5. Mean rates of net leaf CO_2 uptake (A_n) under fatal drought treatments (T7–T9; see Table 1), measured at three times during the experiment. Error bars indicate the standard error of the mean ($n = 3$).

T6 (0.5:3), new tissue was formed almost entirely in roots and none in the stem. When drought intensity was fatal, biomass allocation was only to roots, first at the expense of the stem and later at the expense of the leaves, up to a negative biomass accumulation in stem tissue (see the bar representing T9 (0.25:3) in Figure 3). An average T9 (0.25:3) tree started the experiment with a stem biomass of 2290 mg dry weight and ended it with 2150 mg, a net biomass loss of 140 mg.

Unexpectedly, whereas stem height increased in all trees during the experiment (Figure 1b), stem diameters peaked for some treatments on Weeks 6–10 and shrank continuously thereafter (Figure 4), also reflected by very low to negative stem biomass accumulation (Figure 3). Similarly, leaf area increased during the trial in all trees (data not shown), while in treatments T8 and T9 there was no accompanying increase in leaf biomass. Figure 4 shows that stem diameter decreased in a non-linear fashion, initially increasing up to Week 6, which means that while the net observed stem biomass loss for a T9 (0.25:3) tree was 140 mg, the effective loss was larger (approximation of stem dry biomass on Week 6 was possible since stem density before and after the experiment was similar). Using weekly measurements of stem height and diameter in calculation of stem volume (assuming a conical shape) during the course of the experiment yielded a stem biomass value of 2750 mg for a T9 (0.25:3) tree on Week 6. This means that stem biomass potentially decreased by ~600 mg between Week 6 and the time of mortality. Loss of biomass was partly explained by negative carbon balance between emission of CO_2 in respiration and uptake in photosynthesis. Slow rates of CO_2 emission were found in trees under the highest drought intensity (T7–T9), i.e., ~0.2 μmol m^{-2} s^{-1} at midday (Figure 5) and 0.4 μmol m^{-2} s^{-1} in the late evening in the leaves of T9 (0.25:3) trees. These snapshot measurements were used to approximate the weekly leaf CO_2 exchange (FC, in mg week^{-1}) according to

$$\mathrm{FC} = L_\mathrm{a} \times \mathrm{MW_c} \times (A_\mathrm{n\,fs} \times t_\mathrm{fs} + A_\mathrm{n\,d} \times t_\mathrm{d}) \qquad (6)$$

where L_a is projected leaf area (0.015 ± 0.004 m^2), $\mathrm{MW_c}$ is the molar mass of CO_2 (44 g mol^{-1}), $A_\mathrm{n\,fs}$ and $A_\mathrm{n\,d}$ are net assimilation rates (−0.2 and −0.4 μmol m^{-2} s^{-1}, respectively) under full sunlight (9:00–15:00) and partial sunlight or dark (15:00–9:00) conditions, and t_fs and t_d are cumulative times (in s) of full sunlight and partial sunlight or dark, respectively, along the week. It was estimated, for a first approximation, that ~120 ± 32 mg CO_2 week^{-1} was emitted per tree. Assuming a respiration quotient for carbohydrates of 1.0 and a carbohydrate molar mass of 30 g mol^{-1}, this CO_2 net loss translates into ~81 mg carbohydrates week^{-1}, or a total of ~320 mg stem biomass during the 4 weeks prior to tree mortality. This amount is markedly below the estimated stem biomass loss of 600 mg, suggesting that other processes, including translocations of biomass, also took place. For example, the net biomass accumulation of 460 mg in the root tissue of T9 (0.25:3) trees may have partly relied on reallocation of biomass from the stem.

Hydraulic regulation of different plant organs

We measured traits underlying hydraulic activities for the three main hydraulic components of the trees: changes in root system area; in xylem conductivity; and in stomatal conductance to water vapor. Figure 6 shows that the total area of the root system (A_r) increased in all trees, including trees that suffered the highest drought intensity and did not survive. Based on an initial root area of 5.2 cm^2, a 400% increase in root system area was observed in T1 (0.75:1) and T4 (0.5:1), higher than in the control.

Specific hydraulic conductivity of the xylem, K_s, measured after stems were allowed to rehydrate for 24 h, decreased dramatically with drought, although values varied greatly (see the black bars in Figure 7). K_s decreased by 15, 50, 65 and 75% with increasing drought in T1 (0.75:1), T2 (0.75:2), T4 (0.5:1) and T5 (0.5:2), respectively. The magnitude of reduction in xylem conductivity did not correlate linearly with PDI: for SWC <10% the effect was similar irrespective of irrigation regime, indicating a fixed SWC threshold for loss of xylem conductivity. Loss of K_s could be due to shrinkage of the total volume/diameter of the tracheids or due to embolisms that the plant was

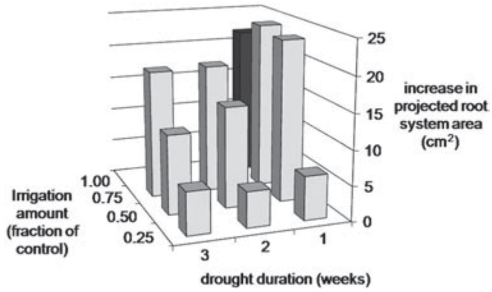

Figure 6. Mean growth in projected root system area in the course of the drought experiment in treatments T1–T9 (see Table 1; $n = 5$–8).

not able to refill during rehydration. In order to distinguish between these processes, we repeated the conductivity measurements after perfusion at high pressure, in which water was forced through the xylem. This treatment presumably refilled embolized tracheids, giving $K_{s\ max}$, which should only be related to the total volume of the tracheids. Indeed $K_{s\ max}$ values for each treatment were higher than K_s values, and had greater uniformity within a treatment. The white bars in Figure 7 show that T1 (0.75:1) trees maintained the $K_{s\ max}$ of control trees and with increasing drought $K_{s\ max}$ dropped by 60–65%, depending on the treatment (and also under fatal drought). This was interpreted as indication that xylem volume decreased following drought, in agreement with measurements of decreased stem diameter under drought (Figure 4).

Leaf stomatal conductance also decreased in response to drought, in relation to PDI:

$$g_s = 0.07 - 0.02 \times \mathrm{PDI}^2 - 0.04 \times \mathrm{PDI} \qquad (7)$$

The effects of drought intensity and duration on g_s (in percent of the control value; see Table 2) were summarized by the regression equations $g_s = 100-25 \times (A_0/A_i)$ $(P < 0.05)$ and $g_s = 100-22 \times (3/D_i)$ $(P < 0.005)$. A reduction of 25% in g_s was observed by reducing water input by 25%. Alternatively, a reduction of 22% in g_s was observed by extending the interval between irrigations by 1 week (Table 2). The second equation also indicated that $g_s = 0$ when $D_i = 0.67$, i.e., one irrigation event in 31.5 days, which is the longest drought duration still allowing stomatal activity in this experiment. Leaf conductance was closely related to leaf water potential (Figure 8): g_s fell as midday leaf water potential declined. g_s was highly correlated with the decrease in SWC ($R^2 = 0.79$; data not shown), and at −2.8 MPa conductance approached zero. Thus, −2.8 MPa is the leaf water potential that resulted in 99% stomatal closure (Ψ99PSC). This tight regulation is characteristic of isohydric plant species.

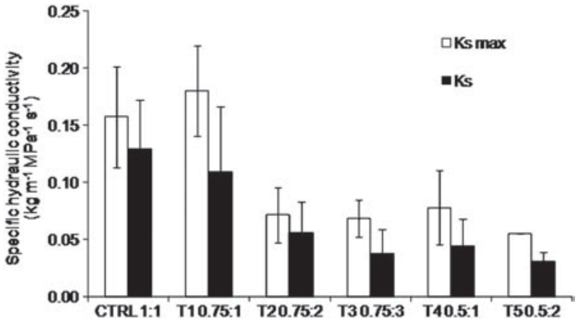

Figure 7. Mean xylem specific and maximal hydraulic conductivity (K_s and $K_{s\ max}$, respectively) in treatments with surviving trees (indexed as shown in Table 1). Error bars indicate the standard error of the mean ($n = 5$–9 for K_s and $n = 1$–4 for $K_{s\ max}$).

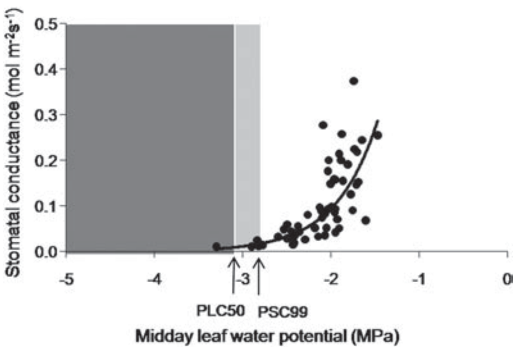

Figure 8. Response of stomatal conductance to water vapor to midday leaf water potential. Data from all drought treatments were obtained from weekly measurements during Weeks 1–8 at midday (each point represents the mean of three replicate measurements). Hydraulic safety margin, between Ψ99PSC and Ψ50PLC, is indicated by light gray background, and PLC > 50 is indicated by dark gray.

Discussion

Hydraulic regulation at the whole tree level

The Ψ99PSC value of −2.8 MPa that we measured for *P. halepensis* is a relatively high value in comparison with other arid coniferous tree species. For example, *Callitris rheomboidea* of Eastern Australia has a Ψ99PSC of −4.3 MPa (Brodribb and Cochard 2009), and *Juniperus scopulorum* of New Mexico, USA has a Ψ99PSC of −5.5 MPa (McDowell et al. 2008). High Ψ99PSC may be related to high sensitivity of the xylem to embolism or to a wide safety margin taken by the plant, since cavitation occurs when Ψ declines below a threshold value. Indeed, in this experiment we found that treatments that resulted in higher loss of xylem conductivity also exposed it to lower midday leaf water potentials (Figure 9). This is in agreement with values reported in the past for *P. halepensis*: 37% PLC at −2 MPa, 48% at −3 MPa and 67% at −4 MPa (Oliveras et al. 2003).

Xylem sensitivity to embolism is often expressed by the Ψ value where 50 percent conductivity loss (Ψ50PLC) occurs. Martinez-Vilalta et al. (2004) listed Ψ50PLC values of 40

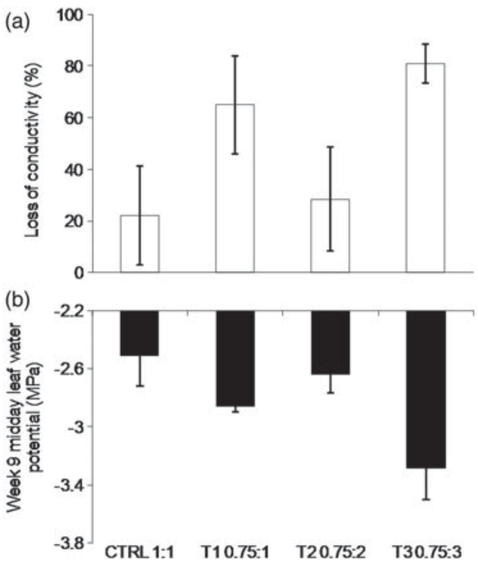

Figure 9. Loss of xylem hydraulic conductivity (%; where PLC = 100 − ($K_s/K_{s\ max}$ × 100)) measured at the end of four drought treatments (indexed as indicated in Table 1; a), and mean midday leaf water potential, measured on Week 8 of the experiment (b). Error bars indicate the standard error of the mean (n = 2–4).

coniferous species; *P. halepensis*, with a Ψ50PLC of −3.11 MPa, ranked at the 9th place, with 80% of the species characterized by lower Ψ50PLC. Tyree et al. (1994) showed a positive relationship between conduit diameter and xylem vulnerability to embolism. Accordingly, a lower Ψ50PLC was expected in the case of *P. halepensis*, where tracheids are only 10 μm in diameter (Oliveras et al. 2003). However, the reported Ψ50PLC of −3.11 MPa (Oliveras et al. 2003) was similar to that estimated from our potted trees (−2.9 MPa) and close to that of other narrow-tracheid pine species. The conductivity loss described in Figure 9 can be linked to xylem cavitation and embolism processes, in turn causing hydraulic dysfunction which may result in tree mortality (Cochard 2006). It is therefore possible that hydraulic failure played a role in the mortality of stressed *P. halepensis* trees, as presented in Figure 10.

The transpiration ratio, T/ET, appears to integrate the intensity and duration effects of the drought, and influences the trees' response to it (Figure 10). In treatments with less frequent but larger irrigation doses, T/ET was 22–24%, while for frequent, smaller water applications, transpiration ratios were as small as 9% (Figure 2). Apparently, even in pot experiments the transpiration ratio is sensitive to water infiltration depth associated with the irrigation dose. This provided a strong link to field measurements. The results of Raz Yaseef et al. (2009) in the Yatir forest showed that small precipitation events were sufficient to maintain the topsoil layer wet during the rainy season, but only more intensive storms infiltrating to the root zone increased T/ET. This demonstrated the importance of precipitation patterns, as opposed to the total amount, on the forest functioning, similar to the results obtained here. The combined greenhouse and field measurements indicate, therefore, that drought effects may be better predicted by assessing its effect on the transpiration ratio than by assessing the absolute amount of water input.

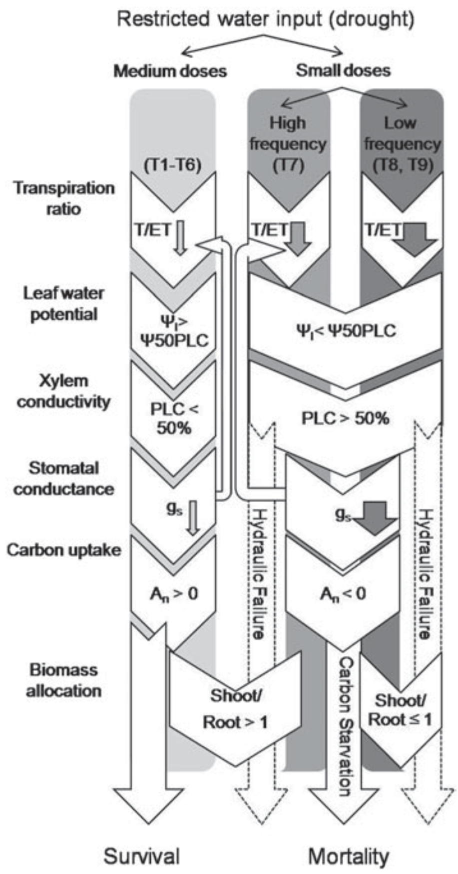

Figure 10. Effects of the main drought scenarios on hydraulic components, carbon management and the tree's fate. Arrow width indicates magnitude of response in T/ET and g_s. Dotted outline indicates a possible pathway without sufficient evidence.

Tree-level hydraulic processes downstream of the transpiration ratio can be described as a cascade of responses, eventually determining the tree's fate (Figure 10). The significance of maintaining Ψ_l above Ψ50PLC is twofold: first, exposing the xylem to extreme tension can result in hydraulic failure; and second, the resulting stomatal closure may lead to carbon loss. Unless the drought stress is relieved, mortality cannot be avoided, despite hydraulic adjustments, such as prioritization of root growth.

Hydraulic safety margin of P. halepensis

The relatively high xylem vulnerability to embolism displayed by trees in this study was not expected in a tree species successfully growing on the dry timberline (Maseyk et al. 2008). Martinez-Vilalta et al. (2004) reported a Ψ50PLC of −9.20 MPa for *C. rheomboidea*, and −7.40 MPa for *J. scopulorum*, both arid coniferous species as well. Notably, while these PLC values are much lower than the value for *P. halepensis*, they are also considerably lower than the values of Ψ99PSC of these exact species, −4.3 and −5.5 MPa, respectively (McDowell et al. 2008). The gap between stomatal closure (Ψ99PSC) and xylem dysfunction (Ψ50PLC) is considered the hydraulic safety margin of the species (Sperry 2004). Note that this gap is very narrow (0.3 MPa) for *P. halepensis* (Figure 8, marked by light gray background), in comparison with the two other species noted above, which are 1.9 and 4.9 MPa, respectively, or 2.4 MPa for the isohydric *Pinus edulis* (Ψ50PLC of −4.5 MPa, Ψ99PSC of −2.1 MPa; Martinez-Vilalta et al. 2004, McDowell et al. 2008).

The significance of the observed narrow safety margin in *P. halepensis* is not clear at present. It is hypothesized that it reflects opposing 'bottom-up' and 'top-down' eco-physiological adjustments. First, these trees, growing in a semi-arid environment and exposed to long seasonal droughts, adopted narrow tracheids and low hydraulic conductance to adjust to soil water availability and the prevailing soil water potential. This likely contributed to the observed trees' low water use and the relatively low mean stomatal conductance. Second, against this background, leaves adapted in order to utilize the maximal operational range available and extended stomatal conductance to CO_2 while avoiding carbon starvation as much as possible, resulting in leaf water potential approaching the 'danger zone' for the hydraulic system. In this respect, *P. halepensis* is more efficient than most tree species in terms of using the carrying capacity of the xylem (Sperry 2004).

If, hypothetically, the hydraulic safety margin of *P. halepensis* was 1.0 MPa wide and as a consequence Ψ99PSC was −2.1 MPa (instead of −2.8 MPa, and assuming Ψ50PLC = −3.1 MPa), stomatal gas exchange would cease as early as Week 4 (instead of Week 11) for T9 (0.25:3) trees, and on Week 8 (instead of ongoing carbon uptake) for T1 (0.75:1) trees. This would inevitably create a negative carbon gain (as shown in Figure 5 for a more advanced stage of the experiment) which could have an immense negative impact on tree survival rate under drought. Is this risky behavior unique to young trees, trying to maximize carbon assimilation during the juvenile phase, while adult *P. halepensis* trees potentially have a wider safety margin? Evidence to the contrary is from leaf water potential values measured in an Aleppo pine forest between October 1998 and May 1999 (Atzmon et al. 2004). There, stomatal gas exchange would not be possible before February if Ψ99PSC was −2.1 MPa. While the latter refers to *P. halepensis* growing in a Mediterranean climate, in a semi-arid forest where $\Psi_l < -2.5$ MPa all year long, the mere existence of this species there would not be possible. A tree species with relatively high xylem vulnerability to embolism like this pine could not survive drought with a wider safety margin. In practice, the semi-arid forest has been relatively highly productive over the past 45 years (Grunzweig et al. 2007, Maseyk et al. 2008, Raz Yaseef et al. 2010), and our pot experiment with the same trees indicates that xylem security was not sacrificed and hydraulic failure was usually avoided due to rapid stomatal responses (Figure 8).

Carbon management in a drought-avoiding tree

The isohydric mode of stomatal regulation indicated by our results suggests that *P. halepensis* is a drought-avoiding species. This strategy inescapably affects CO_2 uptake, and starting in Week 12 in trees under high drought intensity, signs of carbon starvation were observed (negative CO_2 uptake even at midday under optimal light; Figure 5). How can a tree sustain itself without CO_2 uptake? Biomass balance calculations (see Results) show that the loss of biomass in the stem and leaf tissues under acute drought stress (Figure 3) could be explained by CO_2 emission in respiration. Non-structural carbohydrates (NSCs) are used for storage by *P. halepensis* trees (Villar-Salvador et al. 1999) and other pine species (Guehl et al. 1993). Under acute stress associated with stomatal closure, these stored carbohydrates can be used in respiration, thus extending tree survival. Yet it cannot be ruled out that stem biomass in the form of NSCs was also reallocated to the root system, as described in the literature (Callaway et al. 1994, Canham et al. 1999). Our measurements show that there was a significant increase in root biomass of at least 0.46 g in T9 (0.25:3) trees in addition to the initial 1.35 g. This growth took place while stem and leaf tissues were shrinking, which, in turn, coincided with reducing the tree's specific conductivity (Figure 7). Theoretically, a tree exposed to limiting SWC would respond by increasing its root system area while reducing water loss through the canopy. Yet in a situation where stomatal conductance is effectively zero and hence CO_2 uptake is inhibited, the formation of new root tissue cannot rely on newly produced photosynthate and could be supported by reallocation. The carbon budget data (biomass and gas exchange) reported above suggest mobilization of carbohydrates during drought. Thus, the loss of 600 mg from the stem associated with a total net loss of 114 mg from the whole plant indicates translocation of C from the stem, and the persistent increase in root system area with drought further indicates that the target for this translocation was in the roots. This further suggests development of whole tree-level starvation in water-stressed saplings rather than the carbon mobilization disorders hypothesized by Sala et al. (2010). Furthermore, biomass balances of T8 (0.25:2) and T7 (0.25:1) trees, which also died during the experiment, show an effective stem biomass loss of 630 and 900 mg, respectively. These higher losses can be related to the respective size of carbon reserve: the maximal estimated stem biomass (which was 2750 mg in a T9 (0.25:3) tree) was 2930 and 3800 mg in T8 (0.25:2) and T7 (0.25:1) trees, respectively. This indicates that irrespective of the drought scenario, all dying trees showed a negative carbon balance as well as mobilization of carbon resources.

Relevance of greenhouse experiments to the Aleppo pine forest ecosystem

An ongoing research program has been operated for the past decade in a *P. halepensis* dominated afforestation in Yatir, Israel, in the framework of Fluxnet (www.fluxnet.ornl.gov/fluxnet/). This program included several eco-physiological field studies of the Aleppo pine forest ecosystem, in aspects of phenology, hydrology and productivity under drought (Grunzweig et al. 2007, Maseyk et al. 2008, Raz Yaseef et al. 2010, Rotenberg and Yakir 2010). While such field studies are important, they inherently involve too many variables to study mechanisms. Therefore, observed phenomena promote studies of specific effects that require investigation under controlled conditions. The greenhouse provides such a semi-controlled experimental system that allows process-based and manipulation experiments. Yet uncertainties with respect to the extent the saplings' responses represent those of mature trees in the forest require care, when results are extrapolated back to the field. For example, young trees may show different functional and structural responses than adult trees, which include the hydraulic adjustments.

To minimize these effects, precautions were taken in the design of the experiment, e.g., we used young trees (rather than seedlings) and pots fitted to root system volume. The results presented above provided several indications that the greenhouse experiment was consistent with field measurements. For example, an association between leaf water potential and the loss of xylem conductivity in this trial (Figure 9) yielded a Ψ50PLC of approximately −2.90 MPa, which is close to the value of −3.11 MPa reported for field measurements (Oliveras et al. 2003). Rates of net assimilation (A_n) and stomatal conductance (g_s), as well as their interactions, closely matched those measured in the field on the same tree species (Maseyk et al. 2008). A strong dependence of the T/ET ratio on the irrigation amount (Figure 2) corresponded well with observations of a similar association between the field T/ET ratio and the patterns of rain events (Raz Yaseef et al. 2010). These and other results from this experiment clearly demonstrated its relevance to the natural forest ecosystem.

Acknowledgments

We wish to thank Dr Ami Zehavi and Ms Ahuva Daniel of KKL-JNF, Israel, for providing the plant material. We thank Prof. Amram Eshel of Tel Aviv University, Dr Gilboa Arye and Dr Eyal Rotenberg of the Weizmann Institute of Science for scientific advice.

Funding

Jewish National Fund—Keren Kayemet L'Isarel (Alberta-Israel program 90-9-608-08); Global Change and the Hydrological Cycle (GLOWA—Jordan River project 01-2061); Cathy Wills and Robert Lewis Program in Environmental Science; France-Israel High Council for Research Scientific and Technological Cooperation (project 3-6735).

References

Allen, C.D., A.K. Macalady, H. Chenchouni et al. 2009. A global overview of drought and heat-induced tree mortality reveals emerging climate change risks for forests. For. Ecol. Manage. 259:660–684.

Atzmon, N., Y. Moshe and G. Schiller. 2004. Ecophysiological response to severe drought in *Pinus halepensis* Mill. trees of two provenances. Plant Ecol. 171:15–22.

Awada, T., K. Radoglou, M.N. Fotelli and H.I.A. Constantinidou. 2003. Ecophysiology of three Mediterranean pine species in contrasting light regimes. Tree Physiol. 23:33–41.

Ayers, R.S. and D.W. Westcot. 1985. Irrigation water quality criteria. Lewis Publishers, Chelsea MI.

Boyer, J.S. 1982. Plant productivity and environment. Science 218:443–448.

Breshears, D.D., N.S. Cobb, P.M. Rich et al. 2005. Regional vegetation die-off in response to global-change-type drought. Proc. Natl Acad. Sci. USA 102:154144–154148.

Brodribb, T.J. and H. Cochard. 2009. Hydraulic failure defines the recovery and point of death in water-stressed conifers. Plant Physiol. 149:575–584.

Calamassi, R., G. Della Roccaa, M. Falusia, E. Paolettib and S. Stratib. 2001. Resistance to water stress in seedlings of eight European provenances of *Pinus halepensis* Mill. Ann. For. Sci. 58:663–672.

Callaway, R.M., E.H. DeLucia, E.M. Thomas and W.H. Schlesinger. 1994. Compensatory responses of CO_2 exchange and biomass allocation and their effects on the relative growth rate of ponderosa pine in different CO_2 and temperature regimes. Oecologia 98:159–166.

Canham, C.D., R.K. Kobe, E.F. Latty and R.L. Chazdon. 1999. Interspecific and intraspecific variation in tree seedling survival: effects of allocation to roots versus carbohydrate reserves. Oecologia 121:1–11.

Christensen, J.H., B. Hewitson, A. Busuioc et al. 2007. Regional climate projections. *In* Climate Change 2007: The Physical Science Basis. Contribution of Working Group I to the Fourth Assessment Report of the Intergovernmental Panel on Climate Change. Eds. S. Solomon, D. Qin, M. Manning, Z. Chen, M. Marquis, K.B. Averyt, M. Tignor and H.L. Miller. Cambridge University Press, Cambridge, UK and New York, NY, pp 847–940.

Ciais, P., M. Reichstein, N. Viovy et al. 2005. Europe-wide reduction in primary productivity caused by the heat and drought in 2003. Nature 437:529–533.

Cochard, H. 2006. Cavitation in trees. C. R. Physique 7:1018–1026.

Ferrio, J.P., A. Florit, A. Vega, L. Serrano and J. Voltas. 2003. Δ13C and tree-ring width reflect different drought responses in *Quercus ilex* and *Pinus halepensis*. Oecologia 442:512–518.

Flexas, J., J. Bota, F. Loreto, G. Cornic and T. Sharkey. 2004. Diffusive and metabolic limitations to photosynthesis under drought and salinity in C3 plants. Plant Biol. 6:269–279.

Grunzweig, J.M., I. Gelfand and D. Yakir. 2007. Biogeochemical factors contributing to enhanced carbon storage following afforestation of a semi-arid shrubland. Biogeosciences 4:891–904.

Guehl, J.M., A. Clement, P. Kaushal and G. Aussenac. 1993. Planting stress, water status and non-structural carbohydrate concentrations in Corsican pine seedlings. Tree Physiol. 12:172–183.

Holbrook, N.M., M.J. Burns and C.B. Field. 1995. Negative xylem pressures in plants: a test of the balancing pressure technique. Science 270:1193–1194.

IPCC. 2001. Climate change 2001: the scientific basis. Contribution of Working Group I to the Third Assessment Report of the Intergovernmental Panel on Climate Change. Cambridge University Press, Cambridge.

Maestre, F.T. and J. Cortina. 2004. Are *Pinus halepensis* plantations useful as a restoration tool in semiarid Mediterranean areas? For. Ecol. Manage. 198: 303–317.

Martınez-Vilalta, J., A. Sala and J. Piñol. 2004. The hydraulic architecture of Pinaceae—a review. Plant Ecol. 171:3–13.

Maseyk, K.S., T. Lin, E. Rotenberg, J.M. Grünzweig, A. Schwartz and D. Yakir. 2008. Physiology-phenology interactions in a productive semi-arid pine forest. New Phytol. 178:603–616.

McDowell, N.N., W.T. Pockman, C.D. Allen et al. 2008. Mechanisms of plant survival and mortality during drought: why do some plants survive while others succumb to drought? New Phytol. 178:719–739.

Miyamoto, S., I. Martinez, M. Padilla, A. Portillo and D. Ornelas. 2004. Landscape plant lists for salt tolerance assessment. USDI Bureau of Reclamation.

Mueller, R.C., C.M. Scudder, M.E. Porter, T.R. Talbot, C.A. Gehring and T.G. Whitham. 2005. Differential tree mortality in response to severe drought: evidence for long-term vegetation shifts. J. Ecol. 93:1085–1093.

Oliveras, I., J. Martínez-Vilalta, T. Jimenez-Ortiz, M.J. Lledó, A. Escarré and J. Piñol. 2003. Hydraulic properties of *Pinus halepensis*, *Pinus pinea* and *Tetraclinis articulata* in a dune ecosystem of Eastern Spain. Plant Ecol. 169:131–141.

Quezel, P. 2000. Taxonomy and biogeography of Mediterranean pines (*Pinus halepensis* and *P. brutia*). *In* Ecology, Biogeography and Management of *Pinus halepensis* and *P. Brutia* Forest Ecosystems in the Mediterranean Basin. Eds. G. Ne'eman and L. Trabaud. Backhuys Publishers, Leiden, pp 1–12.

Raz Yaseef, N., D. Yakir, E. Rotenberg, G. Schiller and S. Cohen. 2009. Ecohydrology of a semi-arid forest: partitioning among water balance components and its implications for predicted precipitation changes. Ecohydrology 3:143–154.

Raz Yaseef, N., E. Rotenberg and D. Yakir. 2010. Effects of spatial variations in soil evaporation caused by tree shading on water flux partitioning in a semi-arid pine forest. Agric. For. Meteorol. 150:454–462.

Rotenberg, E. and D. Yakir. 2010. Contribution of semi-arid forests to the climate system. Science 327:451–454.

Royo, A., L. Gil and J.A. Pardos. 2001. Effect of water stress conditioning on morphology, physiology and field performance of *Pinus halepensis* Mill. Seedlings. New For. 21:127–140.

Sala, A., F. Piper and G. Hoch. 2010. Physiological mechanisms of drought-induced tree mortality are far from being resolved. New Phytol. 186:274–281.

Scholander, P.F., H.T. Hammel, E.D. Bradstreet and E.A. Hemmingsen. 1965. Sap pressure in vascular plants: negative hydrostatic pressure can be measured in plants. Science 148:339–346.

Seager, R., M. Ting, I. Held et al. 2007. Model projections of an imminent transition to a more arid climate in southwestern North America. Science 316:1181–1184.

Sperry, J. 2004. Coordinating stomatal and xylem functioning – an evolutionary perspective. New Phytol. 162:568–570.

Sterl, A, C. Severijnes and H. Dijkstra et al. 2008. When can we expect extremely high surface temperatures? Geophys. Res. Lett. 35:L14703.

Tardieu, F. and T. Simonneau. 1998. Variability among species of stomatal control under fluctuating soil water status and evaporative demand: modelling isohydric and anisohydric behaviours. J. Exp. Bot. 49:419–432.

Tognetti, R., M. Michelozz and A. Giovannelli. 1997. Geographical variation in water relations, hydraulic architecture and terpene composition of Aleppo pine seedlings from Italian provinces. Tree Physiol. 17:241–250.

Tyree, M.T. and J.D. Alexander. 1993. Hydraulic conductivity of branch junctions in three temperate tree species. Trees 7:156–159.

Tyree, M.T., S.D. Davis and H. Cochard. 1994. Biophysical perspectives of xylem evolution: is there a tradeoff of hydraulic efficiency for vulnerability to dysfunction? IAWA J. 15:335–360.

Villar-Salvador, P., L. Ocana, J. Penuelas and I. Carrasco. 1999. Effect of water stress conditioning on the water relations, root growth capacity, and the nitrogen and non-structural carbohydrate concentration of *Pinus halepensis* Mill. (Aleppo pine) seedlings. Ann. For. Sci. 56:459–465.

Waring, R.H. and W.B. Silvester. 1994. Variation in foliar $\delta^{13}C$ values within the crowns of *Pinus radiata* trees. Tree Physiol. 14:1203–1213.

West, A.G., K.R. Hultine, K.G. Burtch and J.R. Ehleringer. 2008. Seasonal variations in moisture use in a pinon–juniper woodland. Oecologia 153:787–798.